11(B)-1

2.0 ISI KANDUNGAN

ISSN 0128-0740
Bulletin FKKKSA Jld.(5)No.(2)

Kandungan | Halaman

Stress Around Perforation

Dr. Ariffin Samsuri
Petroleum Engineering Department

Abstract

This paper presents the results of a study into the stress around the perforation system. Finite element models of the main factors associated with a borehole and perforations were generated and subjected to various load regimes. The results show the effects of main parameters on the overall stress around the perforation system.

Introduction

It is known that a reservoir rock is in equilibrium between overburden and pore fluid pressure. When borehole and perforations are created in the productive zone, the reservoir rock stresses are redistributed around the borehole and perforation. According to several invertigators, (1-4) the borehole wall appears to be the weakest area. Therefore, when there is a perforation tunnel within the rock mass, rearrangement of the stress takes place and the surrounding rock must carry the redistributed load. This produces a stress concentration around the perforation tunnel, with maximum on the perforation wall, which corresponds to Jaeger's conclusion on a hollow cylinder. (5,6) This may exceed the peak strength of the rock, causing failure within the rock. This process may produce crushed material on the perforation face or the perforation may totally collapse, causing a reduction in perforated well productivity or sand production.

When that phenomena occurs, the perforating job performs no useful function. The method of approach to the problem is finite element method for determining the stress distribution around the perforation, so that the perforation created is stable.

There is an assumption that rock generally behaves elastically, and the problems in elastic rock, such as a stability study of long horizontal tunnel(6) and borehole (3,5), generally can be solved by considering two dimensional stresses with plane strain conditions. Therefore, in this study, two dimensional models have been generated with the assumption that the rock is linear elastic, homogeneous, isotropic and the problem encountered is a plane strain condition. In addition, there are also models with the assumption that the rock is elasto-plastic. The isoparametric element has been used to model the preforation system. Compression is negative and tension positive.

Model Description

The study examined the following materials and structural properties :

1. Preforation length
2. Perforation diameter
3. Shot density
4. Phasing and pattern
5. Rock material properties
6. Rock stresses, including pore pressure

The finite element method was used to model the perforation system and an extensive material testing programme provided data for the models.

Before the final model geometry was chosen, a number of preliminary models were run to ensure realistic of the results. The models were two dimensional: a section along the length of the perforation from the borehole into the reservoir, and a section across the diameter of the perforation. The diametral sections were modelled by octahedral and circular profiles.

The model represented a vertical section of 12 in. and a depth from the borehole into the formation of 15 in. The perforation length ranges from 3 in. to 12 in. with shot densities varied from 1 to 6 shots per foot, phasing angle of 0^o and 90^o with inline, inplane and spiral patterns. The perforation diameter was varied between 0.15, 0.5, 0.75 and 1 in.

The pore pressure within the formation and completion fluid pressure within the perforation was modelled. This altered the effective stress around the perforation. The borehole was cased and cemented.

Results and Discussion

The stress distribution around the perforation depends on the rock properties, perforation length, shot density, pressure differential, phasing angle and pattern, and perforation diameter. It appears that the critical area around the perforation always occur around the perforation tunnel wall, particularly at the centre of both side walls of the entrance hole or at the intersection between the cement-rock interface and perforation tunnel or at the section of the perforation tunnel where the greatest redistributed stress is located, depending on the combination of those parameters.

The stress around the perforation tunnels is greatest at the tunnel wall, decreasing with distance from the perforation and down to normal levels within 0.5 in. from the perforation tip. In general, stresses begin to increase at about 0.875 in. to 3 in. from the perforation centre, but drastically increase within the first 0.75 in. to 0.875 in. from the perforation centre (thickness of 0.5 in. to 0.625 in.). The 0.5 in. thickness of significant stress redistribution around the perforation corresponds to the average thickness of the perforation damage.[7-13]

Figures 1, 2 and 3 show typical stress distribution along the perforation and across the diameter.

FIGURE 1

STRESSES DIST. ALONG X-AXIS DIRECTION

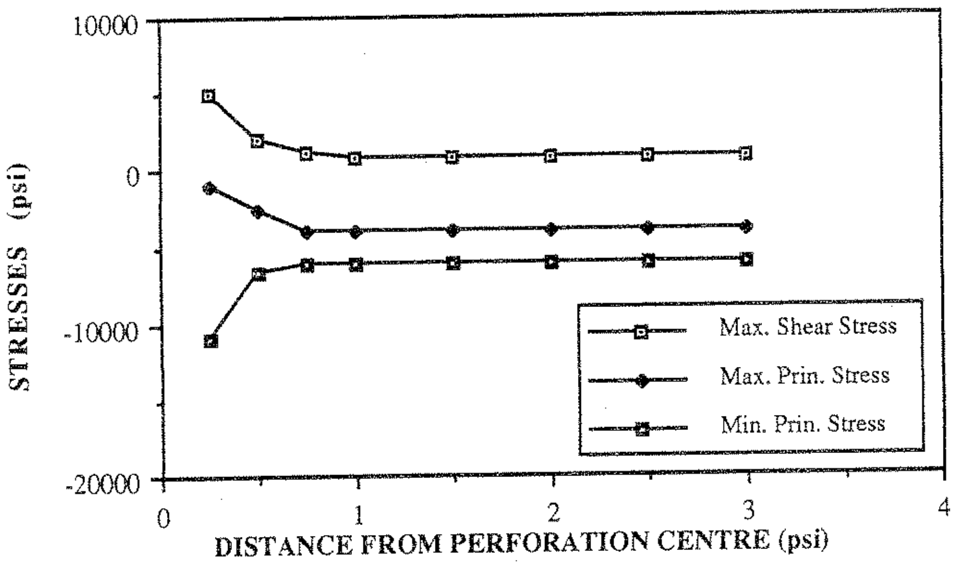

FIGURE 2

STRESSES DISTRIBUTION ALONG THE ROOF

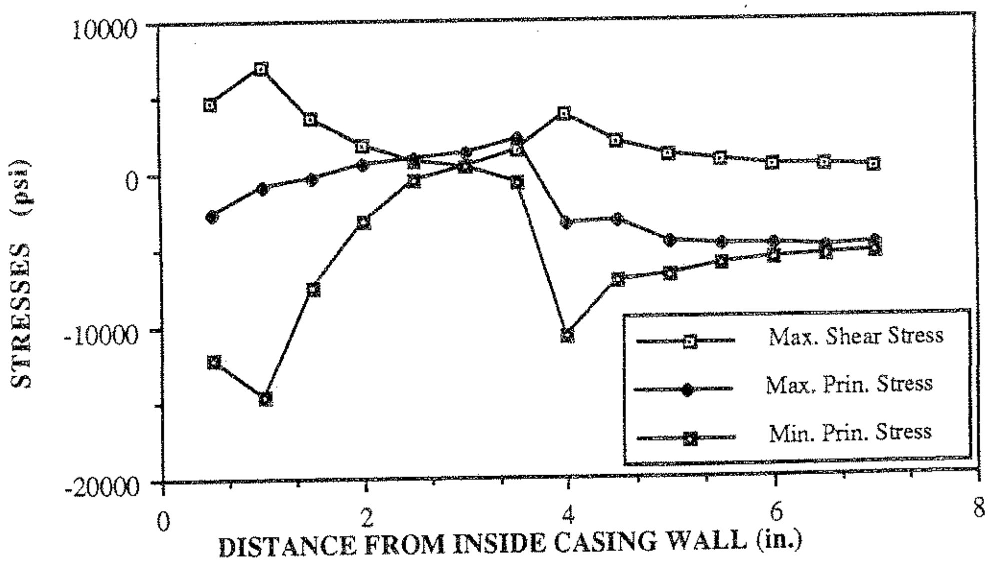

FIGURE 3

MAXIMUM SHEAR STRESS DIST. ALONG X&Y AXES

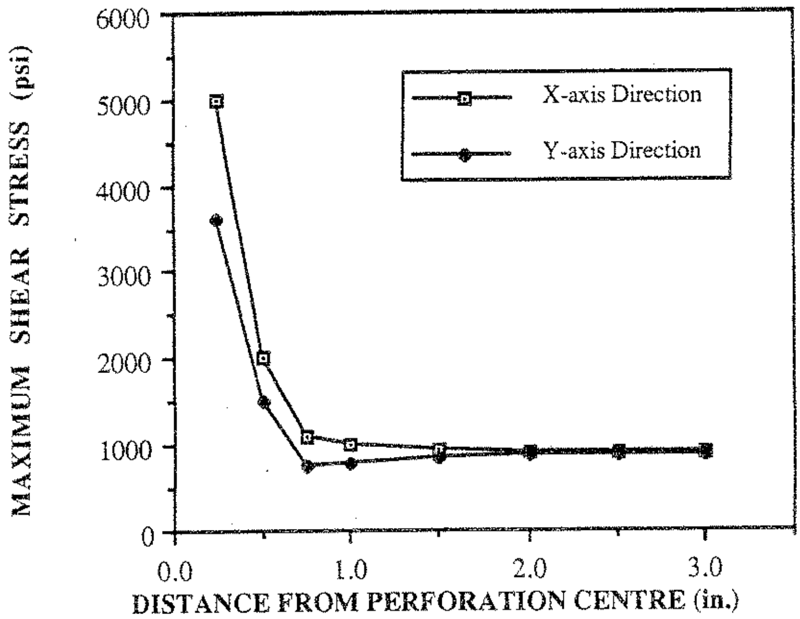

This stress distribution corresponds to the conclusions of Jaeger et. al. (6) and is in agreement with the results on stress distribution around the borehole from previous investigators in borehole stability (2,4,14, 15) and around a circular tunnel.(16) The centre of both side walls of the perforation tunnel appear to be the weakest or critical point from where local fracture or failure will be initiated. These correspond to Terzaghi's rock load classification. (5-6)

The deformation around shot densities greater than 4 shots per foot indicates the development of a plastic zone. The extent of 0.425 to 0.625 in. depends on the stress concentration which is greater for perforations in closer proximity, that is the inline and inplane geometries.

Effect of Rock Properties

The results show that stress distribution around the perforation is independent of the rock mechanical properties but the value is dependent; i.e., distribution would seem to be geometrically dependent. Fig. 4 clearly show that the maximum shear stress around the 0.5 in. diameter, 1 shot per foot perforation is independent of the rock mechanical properties but the maximum shear stress at the critical point depends on the rock mechanical properties.

In general, the maximum shear stress at the critical point decreases as the modulus of elasticity decreases, and as Poisson's ratio and density of the rock increases. These results are understandable since different rock will respond differently to the applied load.

FIGURE 4

EFFECT OF ROCK PROPERTIES ON STRESS

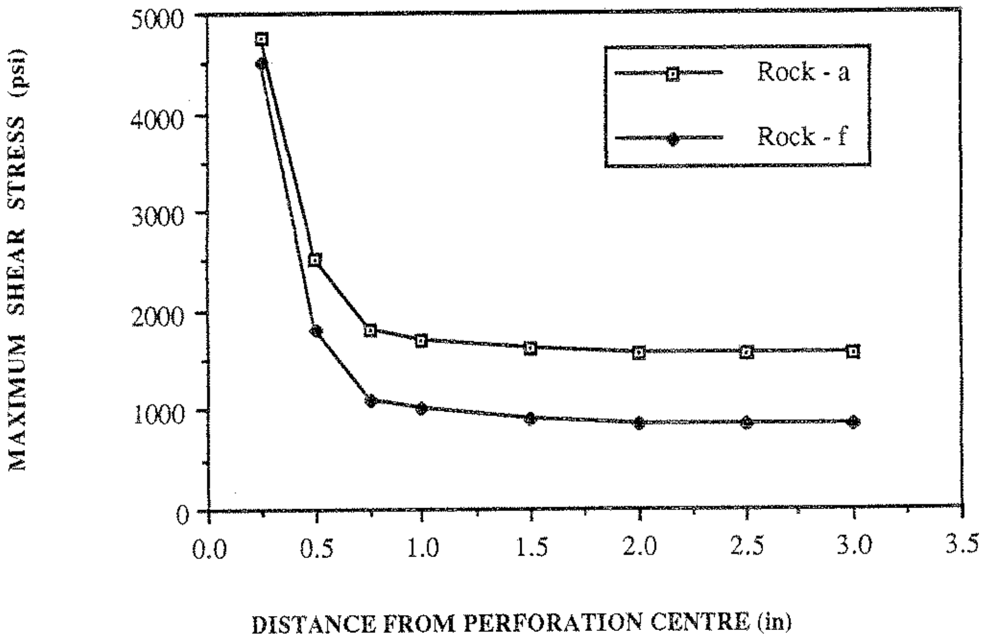

In addition, the stress distribution around the higher shot density perforation (greater than 4 shots per foot) also depends on the behaviour of the rock; i.e., elastic or elasto-plastic, as shown in Fig. 5. The stress around the perforation within the elasto-plastic rock is generally slightly higher than that around the perforation within the elastic rock.

Fig. 5 also shows that there is a plastic zone around the higher shot density perforation. The thickness of this plastic zone depends on the phasing angle and pattern: 0.425 inches for the 0^{o} phasing angle, inline perforation, and 0.625 inches for the 90^{o} phasing angle, spiral perforation or in other words, the thickness of plastic zone increases within the more stable perforation pattern.

FIGURE 5

STRESS DISTRIBUTION ALONG X-DIRECTION

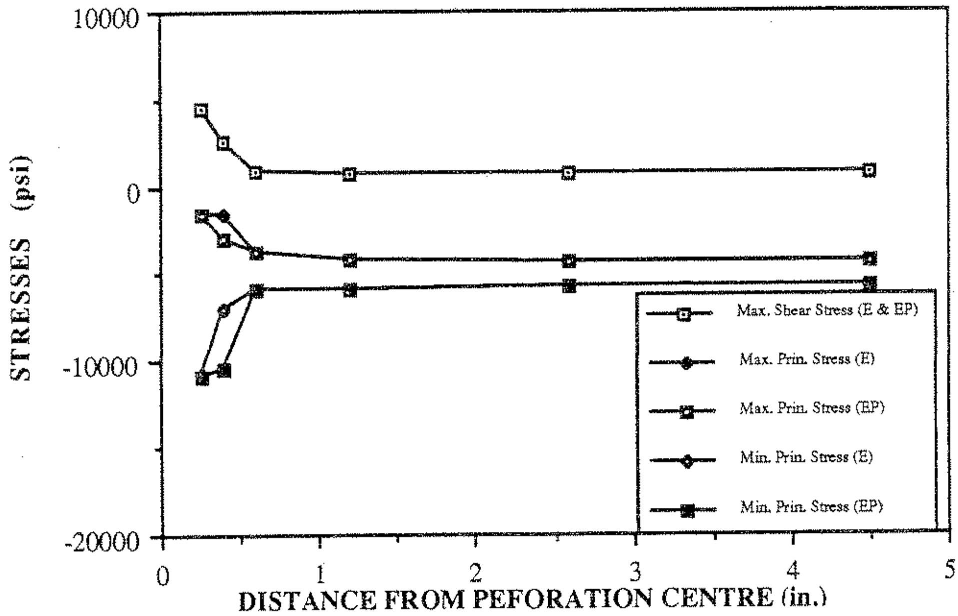

Effect of Perforation Length

It can be seen from Fig. 6 that the stress and strain around the perforation, particularly at the critical point increases as the perforation length increases. This is because the surrounding rock undergoes more load as the perforation length increases. The effect of perforation length on the stress distribution around the perforation becomes more significant as the shot density increases.

Effect of Shot Density

Generally, the stress around the perforation increases as the shot density increases, depending on the phasing angle and pattern. For the shot densities greater than 4 shots per foot, inline perforation, the stress around the top perforation is slightly higher than the lower perforation. The shot density effect on the stress around the perforation becomes significant as the perforation length increases.

Fig. 7 shows a typical plot of stress around the perforation for various shot densities.

FIGURE 6

STRESSES FOR VARIOUS PERFORATION LENGTH

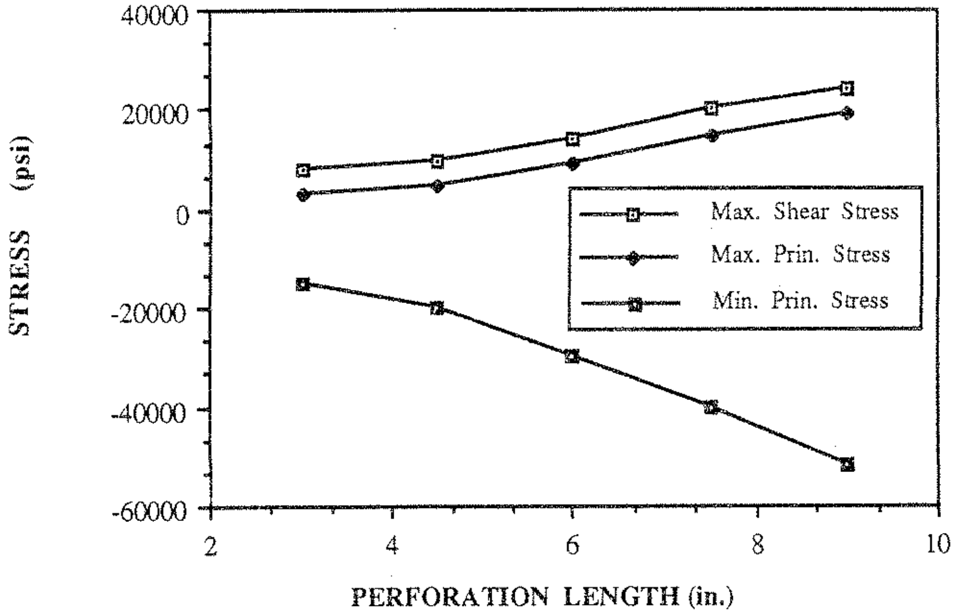

FIGURE 7

STRESSES FOR VARIOUS SHOT DENSITY

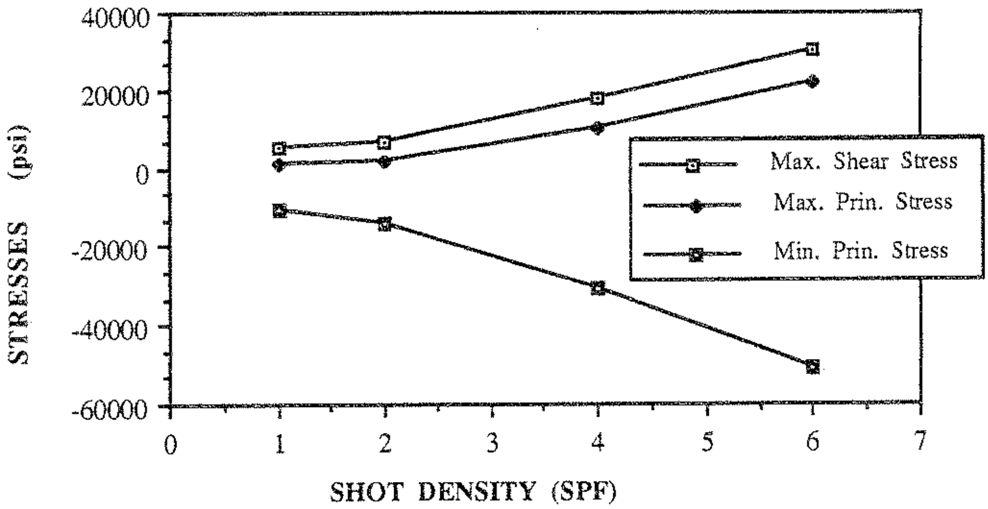

Effect of Pressure Differential

Generally, the stress around the perforation, particularly at the critical point increases as the pressure differential increases, as shown in Fig. 8. The effect becomes more significant as the perforation length and/or shot density increase. In addition, there is a minimum point at around a pressure differential equal to 1000 psi, regardless of the perforation length, shot density, diameter, phasing angle, pattern and rock properties. This is because the surrounding rock around the perforation undergoes more effective overburden load as the pressure differential increases.

FIGURE 8

STRESSES VS PRESSURE DIFFERENTIAL

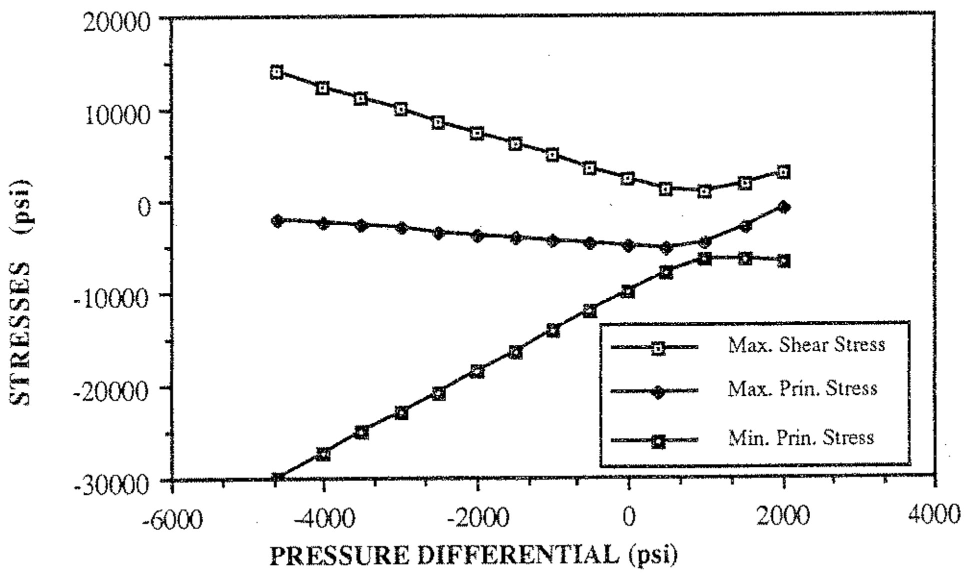

Effect of Phasing Angle and Pattern

In general, the stress around the 0° phasing angle, inline perforation is almost the same as for 90° phasing, inplane perforation. They are slightly higher than stress around the 90° phasing angle, spiral perforation. It appears that stress around the spiral perforation is lower than around the inline or inplane perforation. The stress around the top perforation of inline or spiral pattern is slightly greater than that around the lower perforation since the lower perforations are in a zone of redistributed stress caused by the upper perforation. But, the stress around the inplane perforation is the same, since all perforation are in one horizontal line perpendicular to the applied load, therefore they sustain the same magnitude of effective overburden load.

Effect of Perforation Diameter

The stress around the perforation is slightly increased as the perforation diameter increases. Fig. 9 shows the relationship between stress around the perforation and perforation diameter. From this figure, it can be seen that the diameter effect on the stress around the perforation is less compared with the effect of other factors, particularly perforation length or shot density.

FIGURE 9

STRESSES FOR VARIOUS DIAMETER

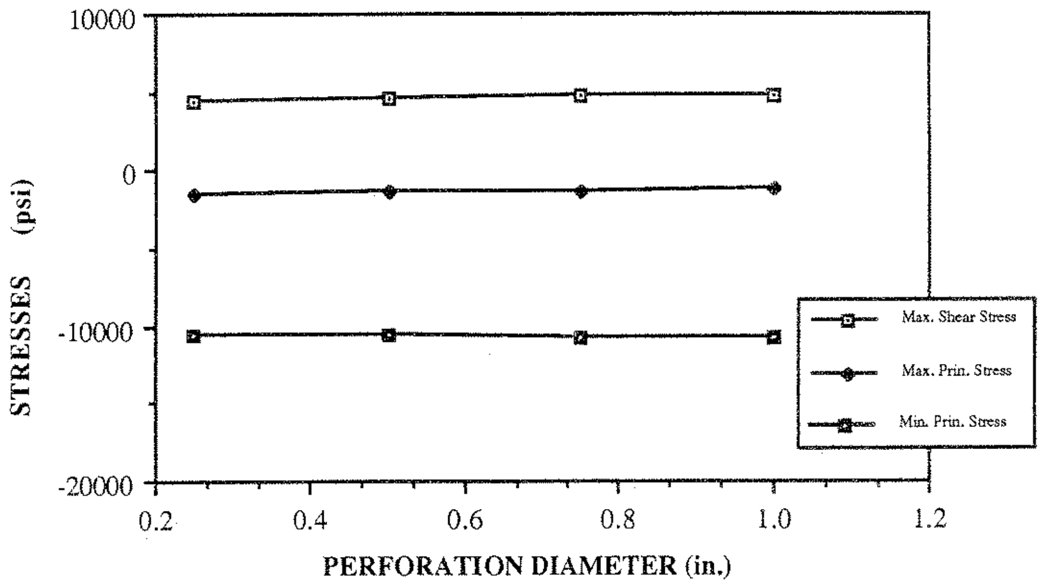

Conclusion

The results from the perforation system finite element models have revealed several characteristics of the stress around the perforation.

1. The stress around the perforation is almost constant after 2 in. from the perforation tip and begins to increase at about 0.875 in. to 3 in. from the perforation centre. The high stress zone always occur around the first 0.5 in. thickness with the highest occuring at the perforation wall, particularly at the critical area, from which failure is always initiated.

2. The critical area always occured at the intersection between the cement-rock and perforation roof, centre of both side walls, perforation roof tip or at the middle of the roof.

3. The stress distribution and the critical area within the perforation wall depend on rock properties, perforation length, shot density, pressure differential, phasing angle and pattern, and perforation diameter.

4. The stress around the perforation increases as the perforation length, shot density, diameter and pressure differential increase. The stress around the spiral perforation is less than around the inplane and inline perforation.

5. The weaker rock generally undergoes more severe deformation than the stronger rock.

6. The effect of diameter is less dominant compared with the other factors, particularly the perforation length and shot density.

7. The shot density effect of the stress around the perforation is more dominant than the perforation length.

Reference

1. W.B. Bradley: "Mathematical Concept - Stress Cloud - Can Predict Borehole Failure", Oil & Gas Journal, vol. 77, no. 8, Feb., 1979.

2. R.K. Bratli & R. Risnes: "Stability & Failure of Sand Arches", SPE Journal, April, 1981.

3. B.S. Aadnoy & M.E. Chenevert, "Stability of Highly Inclined Boreholes", SPE Drilling Engineering, Dec., 1987.

4. W.B. Bradley : "Failure of Inclined Boreholes", Transaction of The AIME, vol. 101, Dec., 1979.

5. J.C. Jaeger & N. G. W. Cook : "Fundamental of Rock Mechanics" 3rd. edition, Chapman & Hall, London, 1979.

6. L. Obert & W. I. Duvall : "Rock Mechanics & The Design of Structure in Rock", John Wiley & Sons Inc., 1967.

7. R.J. Saucier & J. F. Land : "A Laboratory Study of Perforation in Stressed Formation Rocks", paper SPE 5758, Well Completion 5a, vol. I, SPE Reprint Series, 2nd. edition, 1980.

8. Stanley Locke : "An Advanced Method for Predicting the Productivity Ratio of a Perforated Well", Journal of Petroleum Technology, December, 1981.

9. J. A. Klotz, R.F. Krueger & D.S. Pye: "Effect of Perforation Damage on Well Productivity", Well Completion 5a, vol. I, SPE Reprint Series, 2nd. Edition, 1980.

10. M.H. Harris : "How to Estimate Production From Ultradeep Perforation", Oil & Gas Journal, Jan., 1, 1968.

11. Harry, O & Mc. Leod, Jr. : "The Effect of Perforating Conditions on Well Performance", Journal of Petroleum Technology, January, 1983.

12. G. E. King, A.R. Anderson & M.D. Bingham : "A Field Study of Underbalanced Pressure Necessary to Obtain Clean Perforations Using Tubing-Conveyed Perforating", Journal of Petroleum Technology, June, 1986.

13. W.T. Bell, E.F. Brieger & J.W. Harrigan, Jr. : "Laboratory Flow Characteristics of Gun Perforations", Well Completion no. 5a, vol. 1, SPE Reprint Series, 2nd. edition, 1980.

14. R. Risnes, R.K. Bratli & P. Horsrud: "Sand Stresses Around a Wellbore", SPE Journal, December, 1982.

15. Ibid : "Rock Mechanics Applied to the Region Near a Wellbore", proceedings of the 58th. International Congress on Rock Mechanics of International Society for Rock Mechanics, held in Melbourne, 1983.

16. R. E. Goodman : "Introduction to Rock Mechanics", John Wiley & Sons Inc., 1980.